



UNITED NATIONS  
UNIVERSITY

**UNU-GTP**

Geothermal Training Programme

Orkustofnun, Grensasvegur 9,  
IS-108 Reykjavik, Iceland

Reports 2018  
Number 22

## **DEVELOPING A TRAINING SIMULATOR FOR OLKARIA WELLHEAD POWER PLANTS**

**Nathaniel Njeru Mugo**

Kenya Electricity Generating Company Limited  
Olkaria – Off Moi South Lake Road  
P.O. BOX 785 – 20117, Naivasha  
KENYA

*nmugo@kengen.co.ke, nathaniel.njeru@gmail.com*

### **ABSTRACT**

Simulators are an essential part of operator training. Rather than purchasing a full scope high realism simulator, it is possible to develop one to meet specific needs. This project lays the foundation for the development of a training simulator for a 5 MW Olkaria wellhead power plant. This is achieved by building a dynamic model of some of the key power plant elements and running typical simulation scenarios. The outcome of the simulation is promising, showing that the model is yielding results that converge with the behaviour of the power plant, confirming the possibility of developing the training simulator. For implementation, on-site model verification is required with adjustments to the model being made where necessary. Integration of the model with a graphical user interface would also be required.

## **1. INTRODUCTION**

### **1.1 Brief history and development of wellhead power plants**

Kenya Electricity Generating Company (KenGen) operated geothermal power plants that are located in the Olkaria geothermal field in Hell's Gate national park. In the park are located four conventional power plants, namely Olkaria I with an installed capacity of 45 MW, Olkaria II with 105 MW, Olkaria I extension with 150 MW and Olkaria IV with 150 MW. The wellhead power plants consist of 21 units with a combined total effective capacity of 83 MW. In October 2018, Olkaria V was under construction while the rehabilitation of Olkaria I was about to start as well as the construction of an additional unit with a capacity of approximately 80 MW at Olkaria I extension and installation of modular units with a total capacity of around 45 MW. Several more projects are in the planning stage.

### **1.2 The challenge**

Well-trained power plant operators are crucial to ensure smooth running of power plants. Their ability to handle routine operations as well as to respond quickly in emergency situations is a main contributing factor to the security of the company's income as well as to the stability of the power plant operation and the national grid as a whole. For this reason it is of utmost importance that capacity building measures are employed.

One useful tool that is used, are power plant simulators. In KenGen, the conventional power plants have been developed in a structured way and operators have been exposed to different levels of training. The conventional power plants are fairly stable and experience few forced outages. An outage demands quick and determined response from the operators, so a simulator has to be used to expose the operators to outages and ensure that they can react quickly and in a prepared way when a real outage occurs. This has been done in aviation for a long time. There the pilots are exposed to critical situations in simulators, ensuring the they can react quickly and in a determined way to a crisis which they hopefully will never encounter in real life.

The wellhead power plants, on the other hand, are early generation models installed to begin generating fast income from wells that had already been drilled. This has to be seen in context of the lengthy lead time (6-10 years) required to put up a conventional power plant. The wellhead power plants were designed to be modular so that they could be moved when required. Due to their overwhelming success, it has now become economically infeasible to spend a minimum of six months disassembling them, moving them and setting them up in a new location. The expectation is that they run continuously for at least fifteen years. Because of the manner in which they were developed, the training regime was not as rigorous as for the conventional power plants. Additionally, because the plants are located in eight different geographic locations, the number of operators is higher per unit than for the conventional power plants. This increases the logistical complexity of training all the operators. This problem is partially being addressed thanks to a project proposed by a former UNU fellow, who suggested to have centralised monitoring and control of the wellhead power plants. Part of the implementation strategy included the use of training simulators (Apiyo, 2016).

Another challenge was the power evacuation from the wellhead power plants which was initially done using medium voltage 33 kV distribution lines. This issue has been addressed at close to 80% of the wellhead power plants. However, for the remaining 20% coupled with the cyclic nature of the wells this results in more forced outages than at the conventional plants. The capacity of the operators is therefore crucial for quick restoration of the power plants following an outage and for swift but accurate response during disturbances.

### **1.3 Proposed solution and objectives**

Despite the differences between the conventional power plants and the wellhead power plants, it is evident that a training simulator could have a positive impact on the operation of the machines in either of the plant types. This report seeks to investigate the need for a simulator and propose a development/implementation strategy with a special focus on the wellhead power plants and the 5.5 MW wellhead power plants in particular.

## **2. LITERATURE REVIEW**

### **2.1 Investigation on need for simulators**

For a long time, Kenya was dependent on hydro power as a source of electrical energy. Due to their unpredictable hydrological cycle the focus has shifted to geothermal, which has become the base load together with the hydro power plants. Recently, wind power has been emerging. KenGen operates wind power generators with an installed capacity of 25.5 MW. In July 2017, Lake Turkana Wind Power (LTWP) was ready for commercial operation with an installed capacity of 310 MW but was not able to dispatch to the national grid due to delays in completion of the transmission line. During the writing of this report (October 2018), one circuit of the transmission line had been completed and LTWP started dispatching power to the grid. It is likely that the wind turbines will be given dispatch priority. This may

result in geothermal power not being fully dispatched throughout the day as is currently the case, and might result in the necessity to have increased cycling capability.

Indeed, this has been the trend around the world. For various reasons, power plants are required to be flexible in terms of cycling capability with regards to frequent start-ups and shut-downs. This has in turn led to increased automation levels that have reduced the interaction of the power plant operators with the power plant. The less the interaction, the more detailed knowledge about the power plant operation is lost, or, in some cases, never comprehensively obtained (Tomschi et al., 2006). The impact of insufficient operator capacity is not damage of equipment due to the fact that modern power plants have extensive safety and protection systems. Instead, the major impact tends to be reduced availability or generation which affects the income generated by the company (Tomschi et al., 2006).

Even when flexible cycling capability is not required, working under time and pressure constraints can create stress conditions for power plant operators. This applies especially during critical situations, which can lead to cognitive overload, broadly defined as the situation where the volume of information supply exceeds the information processing capacity of an individual (Stemmet and Ahmed, 2015). Simulators can help conditioning the operators to act effectively under such conditions (Vieira et al., 2010). The simulators are therefore essential because they provide plant operators with the opportunity to practise critical scenarios in order to improve their reaction time and response. It also provides an opportune moment to observe operator behaviour, gather information and possibly replicate the performance of the best operators.

## 2.2 Types of simulators

The ANSI/ISA-S77.20-1993 (ISA, 1993) standard categorises Operator Training Simulators (for fossil fuel power plants) into the broad categories described below:

*Generic simulator.* This type of simulator offers a generalised view of the plant and is useful to teach the operators the basic principles of power plant processes but the user interface, automation, control, and even processes may differ from the real plant.

*Full scope, high realism simulator.* This type of system simulates all plant processes including auxiliary systems and dynamic responses of any normal or abnormal operation. Complete functionality of the control and automation system is also implemented in this type of simulator. The operator undergoing the training should not see any difference between the simulator and the real system. This type of simulator is tedious to design, it is very expensive and takes a lot of time to develop (up to three years according to the standard).

*Reduced-scope, high realism simulator.* Simulated process areas are limited to major systems, while auxiliary systems are limited except where relevant for the main operation. The ANSI/ISA standard approximates the lead time as one to two years.

It is this type of simulator that this project wishes to implement to target a specific problem area, in this case start-up, shut-down and load changes.

## 2.3 Simulator development

### 2.3.1 Plant description

The physical parts of the plant are described, using a process flow diagram, control blocks or a combination of two or more methods. Garrido et al. (2009) combine the plant description with a mathematical model whereas Hubel et al. (2017) used a process model based on fundamental equations

combined with a control system model to describe the system and investigate the start-up process. They then developed a simplified schematic of the process models consisting of sub-models. The main objective of the control system model is to show how the power output of the plant is controlled as well as the varying set-points from underlying systems and the separate control loops.

Description of system behaviour using mass and energy balance equations can result in vastly different models because of the complexity of the balance equations. Exact models have specific coefficients that are difficult to define (Hrdlicka et al., 2002).

### **2.3.2 Mathematical model**

A mathematical model of a dynamic system is defined as a set of equations that represent the dynamics of the system fairly well (Ogata, 2010). A system may be represented in many different ways depending on one's perspective. However, no mathematical system can exactly model a physical process (Dulau and Bica, 2014) and different models produce varying results. For instance, when modelling a steam turbine the practice is to simplify the model by omitting several variables and only mapping input variables to outputs. For power plants in general and steam turbines in particular, some inaccuracies can be expected with the mathematical model due to un-modelled dynamics and parametric uncertainties (Chaibakhsh and Ghaffari, 2008). In many cases, flow, pressure, density and other variables are measured or calculated.

Once the equations have been defined it is beneficial to use a tool to create the model and run some simulations.

### **2.3.3 Simulation**

One method is to categorise different incidents and create distinct scenarios. Vieira et al. (2010) extracted from a conceptual model of incident scenarios related to operator error in the electricity industry, and proposed the following:

- Correct action on the wrong object;
- Missing action, based on specified task sequence;
- Inappropriate action (not within task context);
- Additional action, based on specified task sequence; and
- Incomplete task sequence.

### **2.3.4 Validation**

It is important to compare the simulated results to actual measurements. Vieira et al. (2010) proposed the following aspects to look at when evaluating the simulator:

- Correctness and completeness;
- Accuracy;
- Degree of operator immersion in the simulated environment;
- Ease of learning using the simulator; and
- Simulated response time in comparison to real system response time.

### **2.3.5 Graphical user interface**

This is what the operator will see and interact with. It should be similar to the user interface that the operator is accustomed to.

## 2.4 General equations

There are some general equations which are used particularly when modelling power plants. Some assumptions are then made to simplify the equations without compromising the fidelity of the model. In some cases the equations are simplified with the use of measurement data. The generally used equations are listed in the sub-sections below. Specific equations used will be discussed in detail in Section 3.

### 2.4.1 Mass balance equations

The law of conservation of mass states that in a closed system, the mass of the system cannot change over time, that is, the amount of mass remains constant – mass is neither created nor destroyed. The general mass conservation principle for a control volume undergoing a process is shown in Equation 1.

$$\frac{d}{dt} \int_V \rho dV = \sum_i \left( \int_S \rho V_n dS \right)_i - \sum_o \left( \int_S \rho V_n dS \right)_o \quad (1)$$

where  $V$  = Volume (m<sup>3</sup>);  
 $\rho$  = Density inside control volume (kg/m<sup>3</sup>);  
 $S$  = Surface (m<sup>2</sup>);  
 $V_n$  = Fluid velocity normal to surface  $S$  (m/s);  
 $i$  = Input state; and  
 $o$  = Output state.

The mass of any object can be determined by multiplying the volume of the object by the density of the object. The quantity density times area times velocity has the dimensions of mass/time and is called the mass flow rate. Equation 2 shows the common equation used for the steam turbine:

$$V \frac{d\rho_s}{dt} = \dot{m}_{s,i} - \dot{m}_{s,o} \quad (2)$$

where  $V$  = Volume (m<sup>3</sup>);  
 $\rho$  = Density (kg/m<sup>3</sup>);  
 $s$  = Steam; and  
 $\dot{m}$  = Mass flow rate (kg/s);

### 2.4.2 Energy balance equations

The law of conservation of energy is a law of physics that states that energy cannot be created or destroyed but can only be changed from one form into another or transferred from one object to another. In a closed system, the amount of energy is fixed. You cannot create or destroy energy inside the system. But energy can be converted from one form to another (and sometimes back again). Equation 3 shows the general energy conservation principle.

$$\frac{d}{dt} \int_V e\rho dV = \dot{Q} + \dot{W} + \sum_i \left( \int_S e\rho V_n dS \right)_i - \sum_o \left( \int_S e\rho V_n dS \right)_o \quad (3)$$

where  $V$  = Volume (m<sup>3</sup>);  
 $e$  = Energy (J);  
 $\rho$  = Density inside control volume (kg/m<sup>3</sup>);  
 $Q$  = Heat (J);  
 $W$  = Power (J/s);  
 $S$  = Surface; and  
 $V_n$  = Fluid velocity (m/s);

For the steam turbine, the equation can be represented in the form shown in Equation 4.

$$V \frac{d(\rho e)_s}{dt} = (\dot{m}h)_{s,i} - (\dot{m}h)_{s,o} - \dot{W}_s \quad (4)$$

where  $s$  = Steam;  
 $\dot{m}$  = Mass flow rate (kg/s);  
 $h$  = Enthalpy (kJ/kg); and  
 $\dot{W}$  = Shaft power (W).

### 2.4.3 Conservation of momentum

Momentum is defined as the mass of an object multiplied by its velocity. The conservation of momentum law states that, within a problem domain, the amount of momentum remains constant. Momentum is neither created nor destroyed, but only changed through the action of forces as described by Newton's laws of motion. The momentum equation (Equation 5) describes the conditions between the in and out-flow of steam through the control valve (Kim et al., 2001). Equation 6 shows the force acting on the control surface which.

$$V \frac{d(\rho u)_s}{dt} = \dot{m}_{s,i} \dot{u}_{s,i} - \dot{m}_{s,o} \dot{u}_{s,o} + (p_{s,i} - p_{s,o})A + F_s \quad (5)$$

$$F_s = -\frac{1}{2} K_v \rho_{s,i} A u_{s,i}^2 \quad (6)$$

where  $u$  = Velocity normal to control surface (m/s);  
 $p$  = Pressure (Pa);  
 $F_s$  = Force acting on control surface (N);  
 $K_v$  = Valve loss coefficient; and  
 $A$  = Area (m<sup>2</sup>).

### 2.4.4 Stodola's Ellipse Law

The Law of the Ellipse or Stodola's Cone Law provides a method for calculating the highly non-linear dependence of extraction pressure of flow in multistage turbines with backpressure (Cooke, 1985). With this law the mass flow can be related to the inlet and outlet conditions. According to Kim et al. (2001), the condition of a condensing turbine inlet is determined using Stodola Ellipse Law assuming that the condensing pressure is constant. Hubel et al. (2017) uses Equation 7 below to define the Stodola coefficient and Equation 8 to calculate the pressure drop for any load point between 0 and 100% of the nominal steam flow.

$$K_T = \dot{m}_{nom} \times \frac{1}{\sqrt{P_{in,nom} \times \rho_{in,nom}}} \times \sqrt{1 - \left(\frac{P_{out,nom}}{P_{in,nom}}\right)^2} \quad (7)$$

$$\dot{m} = K_T \sqrt{P_{in} \times \rho_{in}} \times \sqrt{1 - \left(\frac{P_{out}}{P_{in}}\right)^2} \quad (8)$$

where  $K_T$  = Stodola coefficient;  
 $P$  = Pressure (Pa); and  
 $nom$  = Nominal values.

### 2.4.5 Control valve equations

The main steam control valve controls the quantity of steam delivered to the steam turbine. Therefore, it plays a critical role in maintaining the turbine speed during no-load conditions and enables the turbine to deal with sudden load variations (Pondini et al., 2017). Equations 5 and 6 show the relationship of steam at the inlet and outlet of the valve. The local pressure loss across the valve is shown in Equation

9 below:

$$\Delta ps = K \frac{\rho V^2}{2} \quad (9)$$

where  $\Delta ps$  = Local pressure loss (Pa);  
 $K$  = Coefficient depending on nature of local resistance;  
 $\rho$  = Density of the fluid (temperature dependent) ( $\text{kg/m}^3$ ); and  
 $V$  = Velocity (m/s).

## 2.5 Model assumptions

According to Sanchez et al. (2013), the following assumptions, which are known to apply to geothermal processes from experimental data, can be used when developing models:

- Flow is uniform in control volume inlets and outlets;
- Turbines and pumps have isentropic efficiencies;
- Kinetic and potential energy changes are negligible;
- The flashing process is accomplished at constant enthalpy; and
- Turbines can only interact with a condenser or directly with a generator.

## 3. DEVELOPMENT OF SIMULATOR

The steps taken to develop a training simulator are as follows:

- Definition of scope;
- Definition of the model;
- Selection of modelling and simulation tool;
- Building the model; and
- Model validation through simulation.

### 3.1 Definition of scope

The scope of this study is to develop the foundation of a dynamic model for a 5.2 MW wellhead power plant. The approach is to focus on the “hot end” of the wellhead power plant and create a simplified geothermal dynamic model. The “hot end” comprises the production well, the main steam system, steam turbine and generator.

### 3.2 Model definition

In order to create a model of the power plant, it is important to get an overview of each system from both the process and control perspective and of each systems’ relationship with other systems.

#### 3.2.1 Plant description

Figure 1 shows the wellhead power plant Olkaria wellhead (OW) 914. There are seven units in this power plant. Units 4 and 5 have two machines, each rated at 3.2 MW and sharing one well. Units, 6, 7 and 8 have one machine rated at 5.5 MW. A single unit uses a single well. Unit 8 has captions showing some of the major components. A brief description of the major systems follows.



FIGURE 1: OW 914 Wellhead power plant

*Steam system.* The geothermal production well produces two-phase fluid, a mixture of steam and liquid (brine). This fluid goes to the separator where the brine is removed from the steam in three steps, gravitational, droplet separation and, finally, mist separation (KenGen, 2015). The goal is to provide dry steam, containing no more than 0.01% brine mist droplets carry-over to the turbine. The wellhead pressure–flow relationship follows a characteristic curve which is unique for each well. However, all the different curves generally show increased flow with decreasing wellhead pressure which corresponds to the typical geothermal well productivity curve for choked well flow (DiPippo, 2005). DiPippo also shows that as the well is opened the flow rate increases quickly while the pressure drops but stabilises eventually, stopping the increase in the flow rate. The well opening is adjusted through a manual valve to provide enough steam for the plant. Any surplus steam which is ideally kept to a minimum is dumped through the silencer to the atmosphere. The brine control valve, which discharges to the silencer, maintains the liquid level in the separator, measured by a level transmitter inside the separator. The steam pressure controller maintains the steam pressure close to a given set-point by routing the excess steam to the silencer. If the steam pressure rises above the set-point, the controller will increase the opening of the steam control valve, directing more steam into the silencer. If the steam pressure decreases, the opposite sequence will occur. The steam controller is configured in such a way that in case of a sudden pressure increase, for example due to a full load rejection, the system can react fast enough to limit the pressure increase. If the controller fails to do so and the steam pressure continues to rise, a rupture disc in the two-phase pipeline between the well and separator break as a final safety measure.

*A steam turbine* is a heat engine which enables the heat energy of steam to be transformed into kinetic energy. It offers many advantages. From the thermodynamic point of view, it can translate a relatively large fraction of the heat energy rendered by the expansion of the steam in the turbine into mechanical work. From the mechanical point of view, the turbine is ideal because the propelling force is applied directly to the rotating element of the driven machine. The steam turbine depends on the dynamic action of steam. The steam pressure drops, heat energy is converted into mechanical kinetic energy, and the steam sets, moving with higher velocity. This high velocity jet of steam then enters the moving blades (fitted on the rotor) of the turbine and experiences a change in direction of motion. This causes a change in momentum which results in an impulse force, converting the kinetic energy of the steam into mechanical work (rotary motion). In order to convert large amounts of energy into useful work with maximum efficiency, it may be necessary to expand the pressure energy of the steam in a series of steps (pressure compounding). Each such step contains a set of nozzles and moving blades and is referred to as stage. A turbine containing two or more stages is known as a multi-stage turbine. The steam enters at one end of the turbine which is known as the steam end and flows axially relative to the rotor to the exhaust end (KenGen, 2015). As mentioned in the earlier section, a control valve is crucial to control the amount of steam being fed into the turbine to match the load and thus maintain constant electrical frequency.



**Condensing system.** The steam condenser condenses steam coming from the turbine exhaust. The condensate is then pumped from the condenser to the cooling tower ensuring that a set-point condenser level is maintained. The level in the condenser is measured by a level transmitter attached to the condenser. The non-condensable gases accompanying the steam are extracted from the condensate via ejectors driven by motive steam from the separator.

The auxiliary cooling water system provides cooling for the condenser gas coolers, generator and lubricating oil coolers. It is designed to run without automation, i.e. the cooling water auxiliary pump and cooling tower fans run continuously at full speed. The auxiliary cooling water pump is manually operated with an on/off switch. A water level sensor in the basin gives alarm annunciations if the water level is too low. Water supply is controlled manually through the use of hand-operated valves adjusted and distributed between the NCG cooler, generator cooler and lubricating oil cooler.

The cooling tower fans are manually operated with on/off switches. Each cooling tower unit has 100% capacity, so all four of them must be running for the condensing system to be on full load. The plant can however be operated at reduced capacity with only three fans running, depending on ambient temperature conditions (KenGen, 2015).

### 3.2.2 Graphical user interface

The goal is to have an interface that matches the one the operators are currently using. Figure 2 shows the current interface.

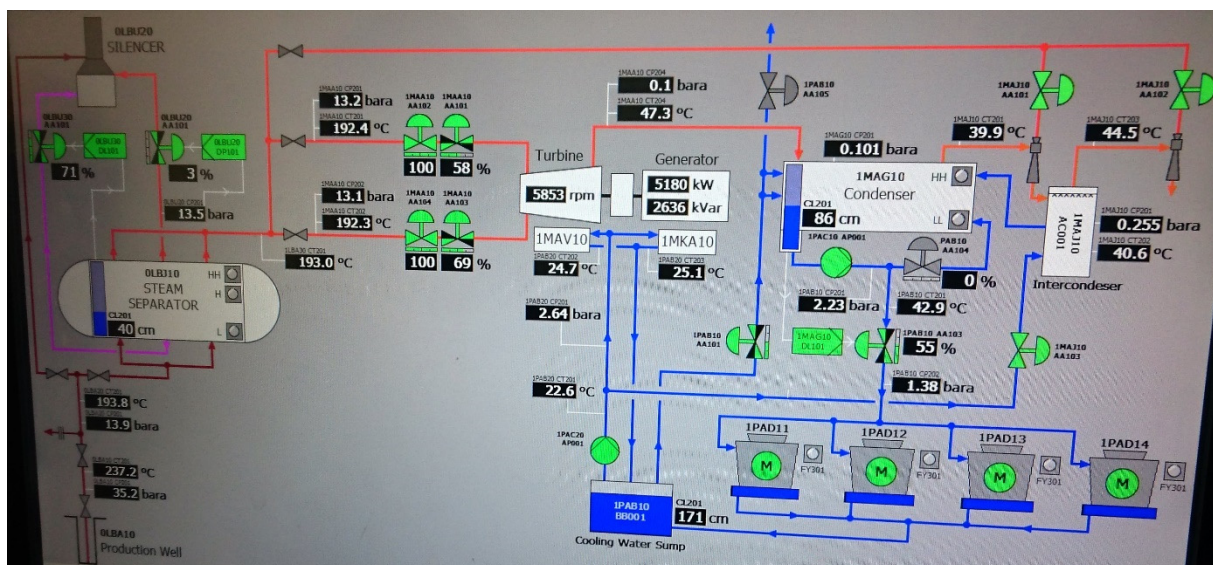


FIGURE 2: Current graphical user interface

Figure 3 is a recreation of the interface drawn with the yEd Graph Editor, a tool for generating diagrams. The diagrams created in yEd can be imported into other software and used in different ways. In this case, the diagram can be integrated with a model to form the interactive part of the simulator.

### 3.3 Selection of modelling tool

The decision was made to use open source software instead of proprietary software. Scilab is free and open source software for numerical computation providing a powerful computing environment for engineering and scientific applications. Like MATLAB, Scilab includes hundreds of mathematical

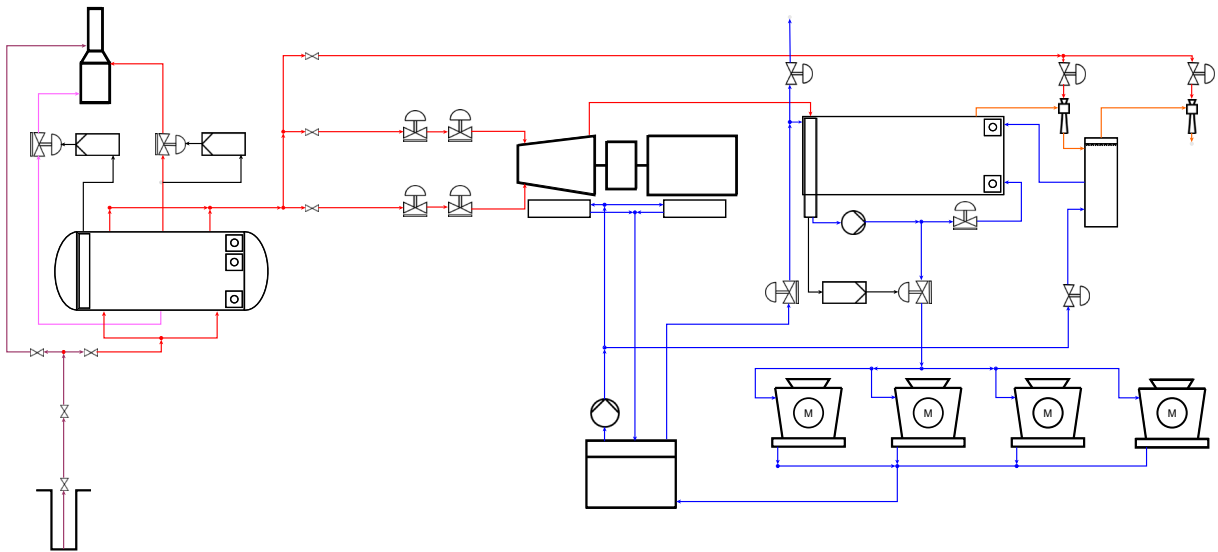


FIGURE 3: Recreation of graphical user interface

functions. It uses a high level programming language allowing the access to advanced data structures as well as 2-D and 3-D graphical functions (Scilab Enterprises, 2012).

Xcos is a graphical editor for modelling and simulation of dynamic (continuous and discrete) systems. It is similar to MATLAB’s Simulink. Xcos provides a modular approach for complex system modelling, using a block diagram editor. Xcos models are compiled and simulated in a single run. The resulting mathematical equations are integrated by a numerical solver with configurable parameters. It is composed of the following main parts:

- *Palettes browser*: All Xcos standard blocks are grouped by categories (signal processing, electrical, hydraulics, derivative, integral, etc.). Figure 4 shows the palettes browser which

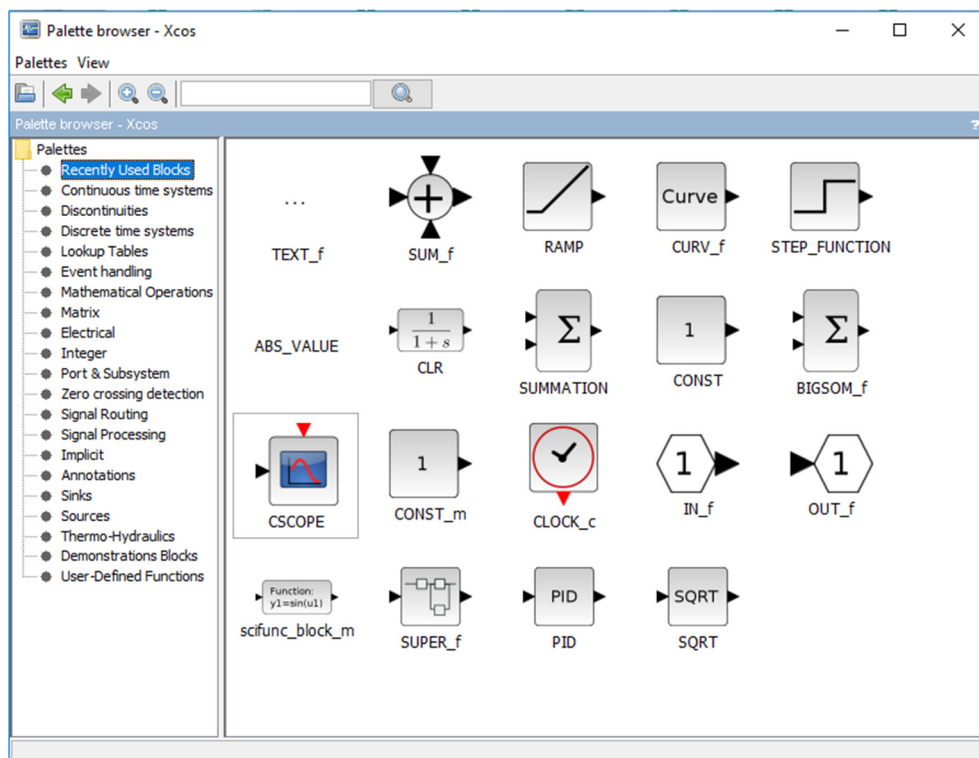


FIGURE 4: Part of Xcos interface

together with the editor forms the main part of the Xcos interface.

- *Editor*: To design flow charts representing a dynamic system made of blocks defined in palettes.
- *Compiler / simulator*: Simulation of complex systems - discrete, continuous, defined by symbolic equations (modelica), etc. and hybrid systems.

Other open source software used was yEd Graph Editor, Inkscape – a vector graphics editor, wxMaxima – a graphical user interface for Maxima, a computer algebra system for the manipulation of symbolic and numerical expressions including differentiation, integration, Laplace transforms, ordinary differential equations, linear equations, polynomials, vectors, matrices and more, and XMind – a mind-mapping and brainstorming software.

### 3.4 Building the model

Figure 5 shows the parts of the power plant that were selected for modelling purposes. The bleed valve represents a means of venting or dumping excess steam, mimicking part of the functionality of the silencer. The pressure control valve and brine level control valve were not included in the model. However, if a functional model of the control valve depicted in Figure 5 can be developed, it could be implemented by making a few minor adjustments.

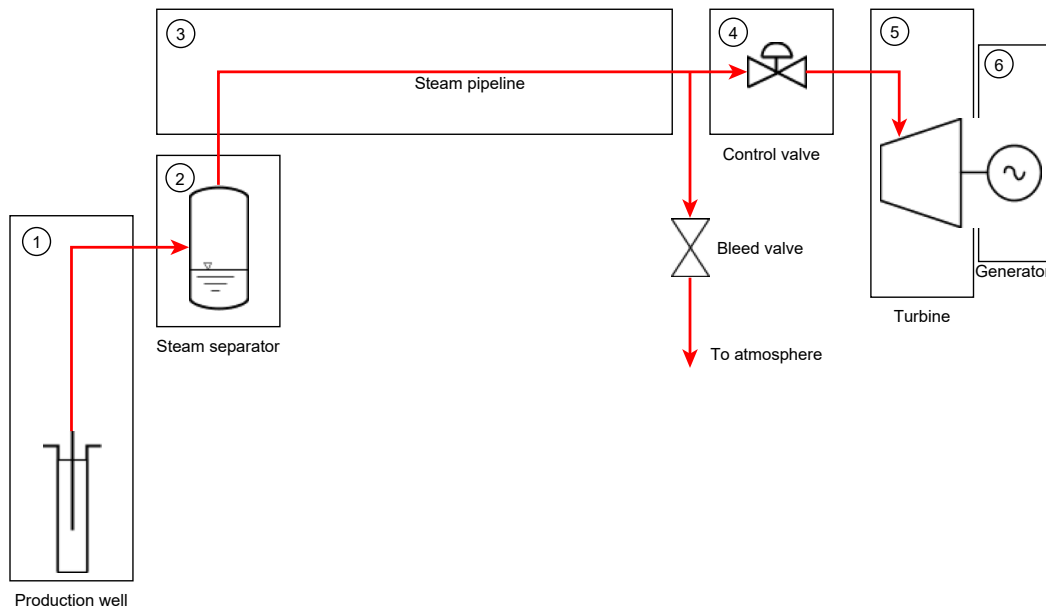


FIGURE 5: Selected systems from power plant for model

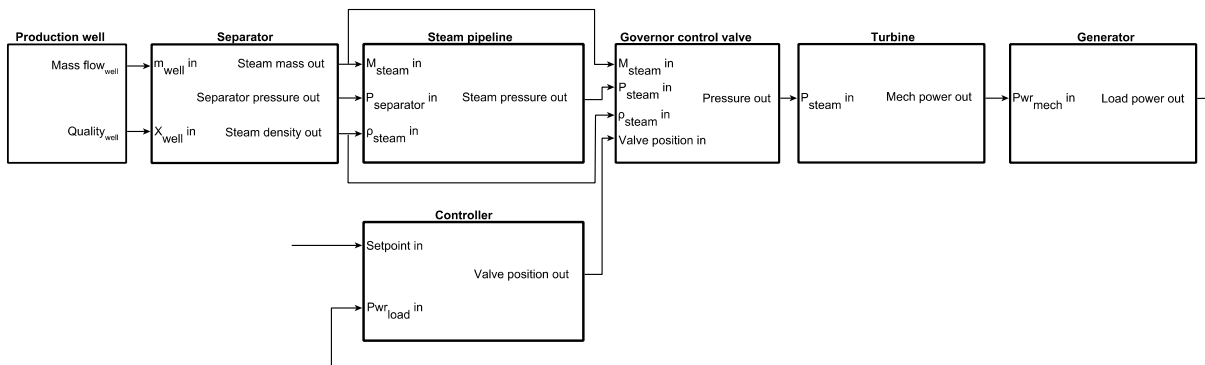


FIGURE 6: Block diagram showing inputs and outputs to each system

The block diagram in Figure 6 shows the major outputs from each system which form inputs into the next system. The systems are discussed in the following sub-sections.

### 3.4.1 Production well

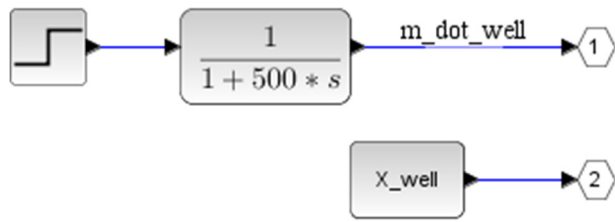


FIGURE 7: Production well in Xcos

Data from one of the production wells was obtained which has two-phase fluid flow of 18.1 kg/s. The characteristic behaviour of the wells differ from one well to another. A time constant of 500 s was assumed. Figure 7 shows the implementation of the production well in Xcos. It consists of a step function with a final value of 18.1 kg/s and a transfer function with a time constant of 500 s. Quality of well ( $X_{well}$ ) is 0.65.

### 3.4.2 Steam separator

It is desired to get separator pressure as the primary output from this block. If the steam density is known, the pressure can be obtained using the steam tables. The density can be calculated from the mass and volume of the steam.

Ignoring the energy balance equation and using only mass balance as shown in Equation 10, we can relate the total mass flow rate of two-phase fluid from the well to the mass of steam in the separator:

$$\frac{d M_s}{dt} = \dot{m}_w X_w - \dot{m}_s \quad (10)$$

where  $M$  = Mass of steam (kg);  
 $s$  = Steam;  
 $w$  = Well; and  
 $X$  = Steam quality.

At time  $t = 0$ ,  $M_s = \dot{m}_w X_w$ . Equations 11, 12 and 13 show the relationship between the steam volume and the level of brine in the separator. The relationship is important as the brine level is a known variable:

$$V_s = V_{sep} - V_b \quad (11)$$

$$V_b = L_b \times A_{sep} \quad (12)$$

$$V_s = (L_{sep} - L_b) \times A_{sep} \quad (13)$$

where  $V$  = Volume ( $m^3$ );  
 $sep$  = Separator;  
 $b$  = Brine;  
 $L$  = Length or level (m); and  
 $A$  = Area ( $m^2$ ).

For normal operation, the separator has a brine level of 0.410 m. Though the external dimensions of the separator were easily retrievable from the separator drawings and data sheets, the internal dimensions were not indicated in the documentation and were therefore estimated. The length was estimated to be 1 m and the area  $2.9 m^2$ . The density of steam can therefore be obtained by dividing mass by volume.

Figure 8 shows the model as implemented in Xcos. For the other systems, fluid properties were obtained using CoolProp which is a free and open-source database that includes pure fluids, pseudo-pure fluids, and humid air properties based on the most accurate formulations in open literature (Bell et al., 2014). For the separator system block the use of the CoolProp library was not possible, so a simple relationship between steam density and separator pressure had to be obtained using different levels of brine in the separator and assuming that the steam mass remains constant. Table 1 shows the pressure for different densities from the steam tables. Figure 9 shows a graphical representation of this relationship.

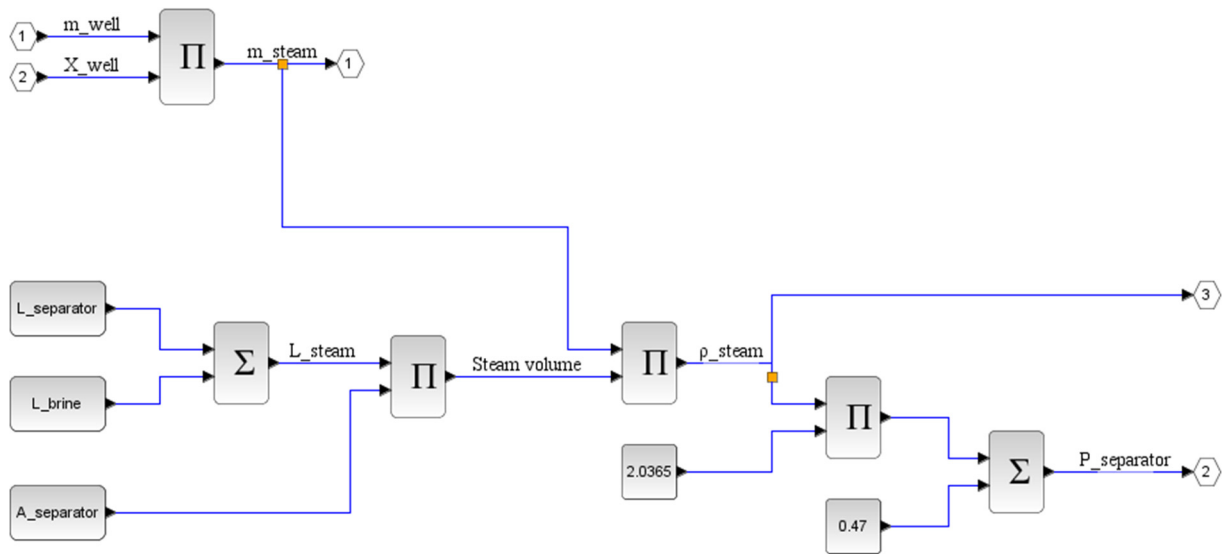


FIGURE 8: Implementation of separator in Xcos

TABLE 1: Pressure-density relationship from steam tables for different brine levels in the separator

Brine level (m)	Steam density (kg/m <sup>3</sup> )	Separator pressure (Pa)
0.28	5.635	10.998
0.35	6.241	12.238
0.41	6.876	13.535
0.53	8.632	17.124
0.68	12.678	25.343

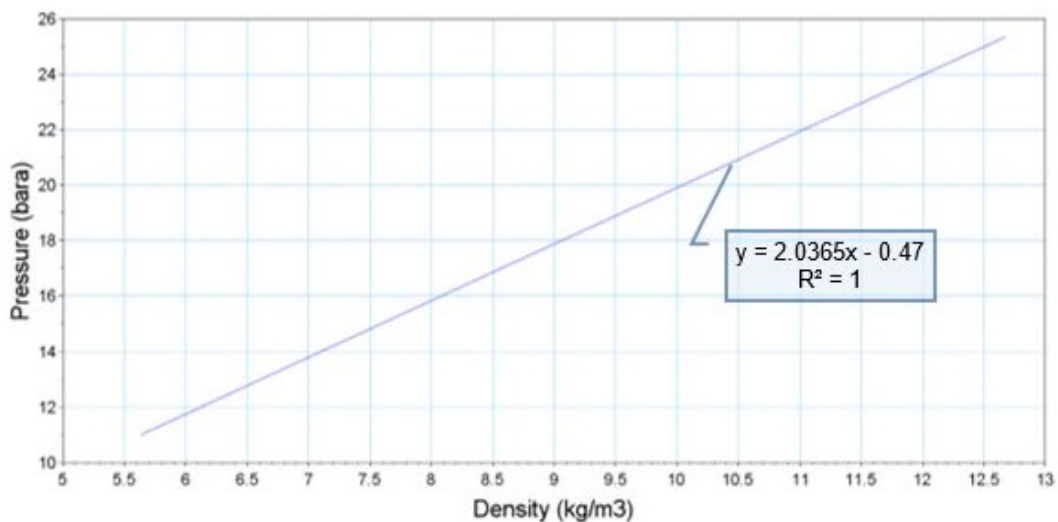


FIGURE 9: Relationship between separator pressure and steam

### 3.4.3 Steam pipeline

The length of the steam pipe varies from ten to twenty metres for the different wellhead power plants. A length of 15 m was used for modelling this part of the system. The diameter of the pipe is 14” (0.3556 m) according to power plant drawings. The Darcy-Weisbach formula shown in Equation 14 was used to calculate the friction losses in the pipe:

$$\Delta P_{friction} = \frac{1}{2} \rho v^2 f \frac{L}{D} \quad (14)$$

where  $\Delta P$  = Pressure drop (Pa);  
 $\rho$  = Density (kg/m<sup>3</sup>);  
 $v$  = Velocity (m/s);  
 $f$  = Friction factor;  
 $L$  = Length (m); and  
 $D$  = Diameter (m).

The Colebrook-White equation (Equation 15) is used to find the friction factor for a Reynolds number greater than 400:

$$\frac{1}{\sqrt{f}} = -2 \log_{10} \left( \frac{\varepsilon}{3.7D} + \frac{2.51}{Re\sqrt{f}} \right) \quad (15)$$

where  $\varepsilon$  = Relative roughness (mm); and  
 $Re$  = Reynolds number.

Due to the implicit form of the Colebrook-White equation, an iterative solution obtained with numerical methods is required to calculate the friction factor. A function written by Dr. Páll Valdimarsson in Scilab was used to calculate the friction factor using a fixed point iteration method. For detail see Appendix I.

The relative roughness is the absolute roughness of the pipe divided by the internal diameter of the pipe. For the model, a diameter of 14" (0.3556 m) was used. Roughness for a new welded carbon steel pipe is 0.05 mm. To account for scaling in the pipe an absolute roughness of 1 mm was used.

To calculate the Reynolds number (Re), Equations 16-19 were used:

$$Re = Vd/\nu \quad (16)$$

$$\nu = \mu/\rho \quad (17)$$

$$V = \frac{Q}{\pi d^2/4} \quad (18)$$

$$Q = \dot{m}/\rho \quad (19)$$

where  $V$  = Velocity of fluid (m/s);  
 $d$  = Internal diameter of pipe (m);  
 $\nu$  = Kinematic viscosity (m<sup>2</sup>/s);  
 $\mu$  = Fluid viscosity (Pa s); and  
 $Q$  = Volumetric flow (m<sup>3</sup>/s).

The fluid density and viscosity were obtained using the CoolProp library with a Scilab script written by Dr. Páll Valdimarsson for conversion to SI units. The frictional losses were found to be around 0.011 bar which is negligible, but the block was nonetheless included in the model as it can still be used for longer steam pipes simply by adjusting the dimensions. Figure 10 shows the implementation of this system in Scilab.

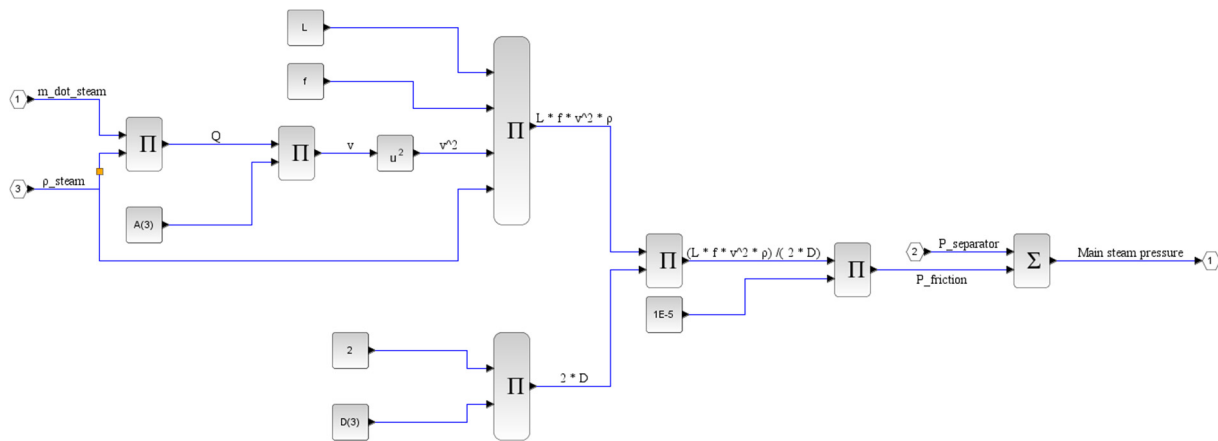


FIGURE 10: Xcos implementation of steam pipeline

### 3.4.4 Governor control valve

The wellhead power plant imitated by the model has two control valves for steam admission. The model, however, assumes only one valve. Equation 20 shows the pressure drop across the valve:

$$P_{in} - P_{out} = \frac{1}{2} \rho v^2 k_l \tag{20}$$

- where  $P_{in}$  = Pressure in to the valve (bar-a);
- $P_{out}$  = Pressure out of the valve (bar-a); and
- $k_l$  = Head loss factor.

It should be noted that this equation is usually used for rigid water column dynamics. The head loss factor was related to the valve position using Equation 21:

$$k_l = \frac{k_{l,min}}{X} \tag{21}$$

- where  $k_l$  = Head loss factor;
- $X$  = Valve position (%); and
- $min$  = Minimum value.

As field data shows, the pressure drop across the valve can vary between 0.5 and 4 bar-a. Rather than calculating the pressure drop, the known data was used and the head loss factor calculated instead. Figure 11 shows the model created for the control valve.

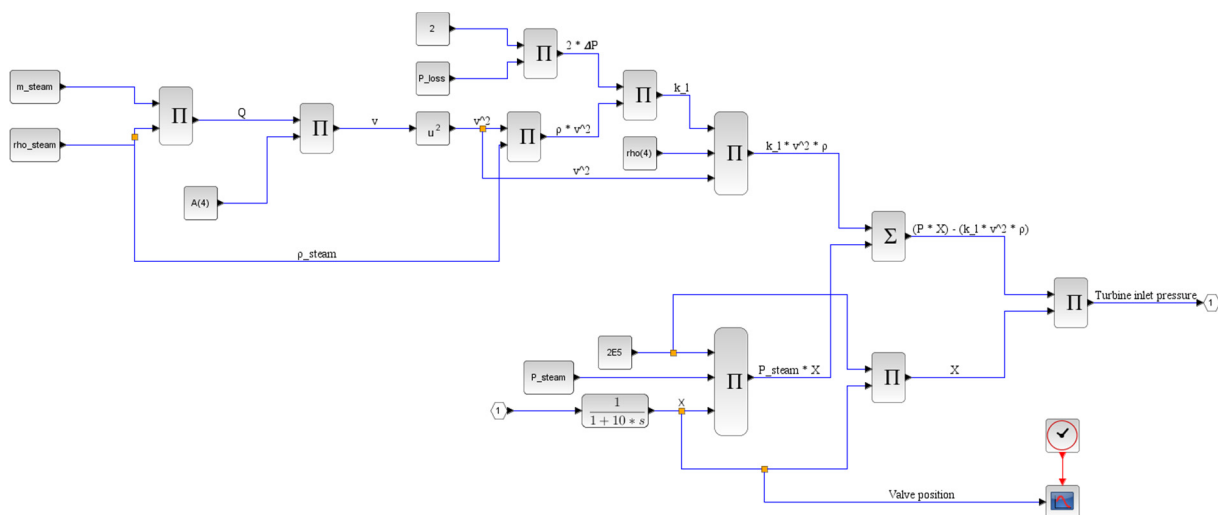


FIGURE 11: Implementation of control valve in Xcos

### 3.4.5 Steam turbine model

Two models were developed. The first was based on simplified versions of Stodola’s ellipse law and the control valve pressure loss equations as well as the energy balance equation, all of which are mentioned in Section 2.4 of this report. Figure 12 shows the implementation in Xcos.

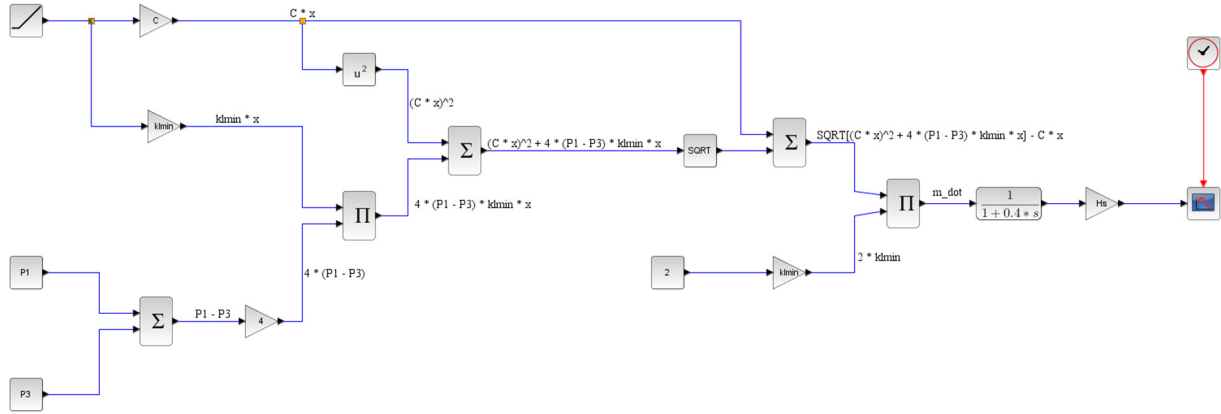


FIGURE 12: Implementation of first turbine model in Xcos

The second model used was adopted from Chaibakhsh and Ghaffari (2008). According to the authors, the relationship between mass flow and pressure drop across the turbine as defined by Stodola in 1927 can be modified to include the effect of inlet temperature ( $T_{in}$ ) as shown Equation 22:

$$\dot{m}_{in} = \frac{K}{\sqrt{T_{in}}} \sqrt{P_{in}^2 - P_{out}^2} \tag{22}$$

where  $\dot{m}_{in}$  = Mass flow rate (kg/s);  
 $K$  = Stodola coefficient; and  
 $P$  = Pressure (MPa).

As demonstrated by Chaibakhsh and Ghaffari (2008), the constant  $K$  can be obtained by plotting the mass flow rate against the pressure drop and temperature at the inlet of the turbine. In this project, such measurement data was not available so  $K$  was assumed to be similar to that. Chaibakhsh and Ghaffari (2008) also plotted output pressure against input pressure and obtained the following transfer function:

$$\frac{P_{out}}{P_{in}} = \frac{0.29475}{0.4s + 1} \tag{23}$$

It is assumed that the time constant is 0.4 s. By assuming that the steam expansion in the turbine is adiabatic and isentropic, the ideal gas pressure-temperature relation as shown in Equation 24 holds true:

$$\frac{T_{out}}{T_{in}} = \left(\frac{P_{out}}{P_{in}}\right)^{\left(\frac{k-1}{k}\right)} \tag{24}$$

where  $k$  =  $C_p/C_v$ , polytrophic expansion factor;  
 $C$  = Specific heat (kJ/kg K);  
 $p$  = Constant pressure; and  
 $v$  = Constant volume.

Equation 25 shows the form of the energy equation which relates power output to steam energy decline in a turbine:



$$W = \eta \dot{m}(h_{in} - h_{out}) = \eta C_p \dot{m}(T_{in} - T_{out}) \tag{25}$$

where  $W$  = Power (MW);  
 $\eta$  = Efficiency;  
 $h$  = Enthalpy (kJ/kg);  
 $C$  = Specific heat (kJ/kg K); and  
 $p$  = Constant pressure.

Combining Equations 24 and 25, we obtain Equation 26:

$$W = \eta C_p \dot{m}(T_{in} + 273.15) \left( 1 - \left( \frac{P_{out}}{P_{in}} \right)^{\frac{k-1}{k}} \right) \tag{26}$$

Figure 13 shows the implementation of the Chaibakhsh and Ghaffari (2008) turbine model in XCos where  $K_1 = 480$  and  $K_2 = (\eta \times C_p)/1000 = 1.942 \times 10^{-3}$ . The specific heat value used was 2.1581. It should be noted that some of their model parameters were derived from a set of 650 data points for different steady state and transient conditions. Some of the values in this model are different. The wellhead turbine unit efficiency was assumed to be 90% and the  $K_1$  value was assumed to be lower. The value in Equation 23 was changed from 0.29475 to 0.405.

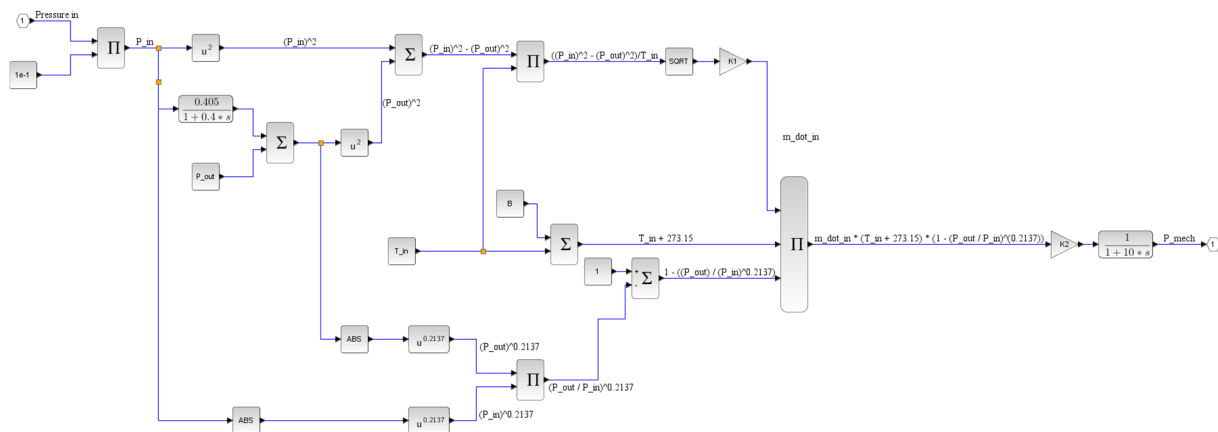


FIGURE 13: Implementation of second turbine model in Xcos

The exact model produced an instantaneous result in case of full load operation, probably caused by the lack of a control valve and due to static values used for temperature and other constants. A transfer function with a time constant of 10 s was added to rectify this instantaneous response and get a more realistic dynamic response.

### 3.4.6 Synchronous generator

Electrical power can be captured as shown in Equation 27:

$$P_e = \left( \frac{UV}{x_d} \right) \sin(\delta) \tag{27}$$

where  $P_e$  = Electrical power (MW);  
 $U$  = Excitation voltage (V);  
 $V$  = Terminal voltage (V);  
 $x_d$  = Direct axis synchronous reactance ( $\Omega$ ); and  
 $\delta$  = Rotor angle.

Neglecting losses, torque, frequency and droop characteristics, the generator equations were simplified

and Equation 28 below was used:

$$P_l = P_m - P_e \quad (28)$$

where  $P_l$  = Load power (MW);  
 $P_m$  = Mechanical power (MW); and  
 $P_e$  = Electrical power (MW).

Figure 14 shows the model developed using this equation. More work is required to strengthen the model of the synchronous generator. The final values for excitation voltage and terminal voltage were 110 V and 11 kV, respectively. The rotor angle was assumed to be  $30^\circ$  and the direct axis synchronous reactance was 1.1. A time constant of 10 s was also assumed.

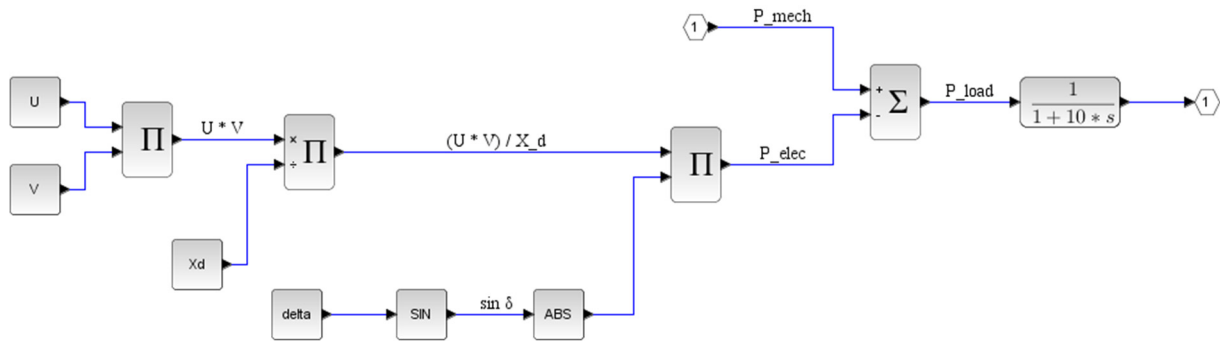


FIGURE 14: Implementation of generator model in Xcos

### 3.4.7 Controller

The model was based on the assumption that the generator is connected to an infinite bus. In such a case, the controller regulates only the power (Chaibakhsh and Ghaffari, 2008). The model consists of a comparator that subtracts the feedback signal from the set-point value. The error signal is fed to a pre-defined Xcos PID controller. Equation 29 shows a typical expression of the PID controller (Garrido et al., 2009).

$$u = P + I + D = K_p e + \frac{K_p}{T_i} \int e dt - T_d \frac{dy_f}{dt} \quad (29)$$

where  $u$  = Control signal;  
 $P$  = Proportional;  
 $I$  = Integral;  
 $D$  = Derivative;  
 $K_p$  = Proportional gain;  
 $e$  = error;  
 $T_i$  = Integral time constant;  
 $T_d$  = Derivative time constant; and  
 $y_f$  = Low pass filter.

For the wellhead power plant a PI controller is used so the derivative value in the Xcos block could be set to zero. Figure 15 shows the implementation of the controller in Xcos.

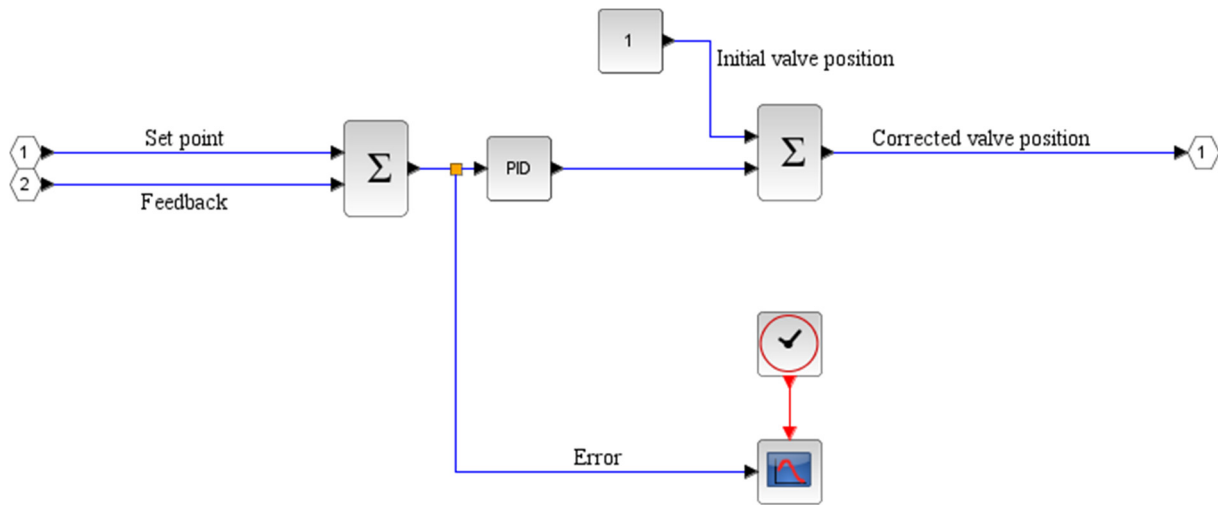


FIGURE 15: Implementation of controller in Xcos

#### 4. SIMULATION RESULTS AND ANALYSIS

Figure 16 shows the overall system implementation of the hot end of the wellhead power plant which individual parts have been described in Section 3. The calculation of the steady-state operation of the power plant was carried out using a script written in Scilab. Changes were made where necessary. The final script that was used is shown in Appendix I.

The model was subjected to three different simulation scenarios, namely:

- Start-up;
- Set-point change; and
- Adjustment of controller parameters.

The results are shown in the subsequent sub-sections with a brief analysis and discussion.

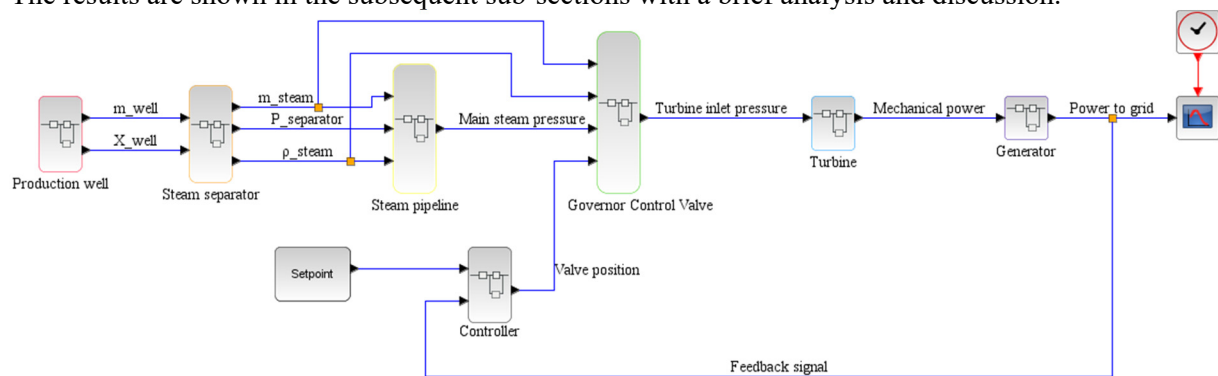


FIGURE 16: Overall system implementation in Xcos

#### 4.1 Start-up

Well flow is started by opening the master valve followed by gradual opening of the main steam valve (located at the well, not to be confused with the emergency shut-off valve or main steam isolation valve situated before the governor control valve) until operation pressure is reached. This usually takes 60 minutes. Figure 17 shows the simulated results of the production well flow.

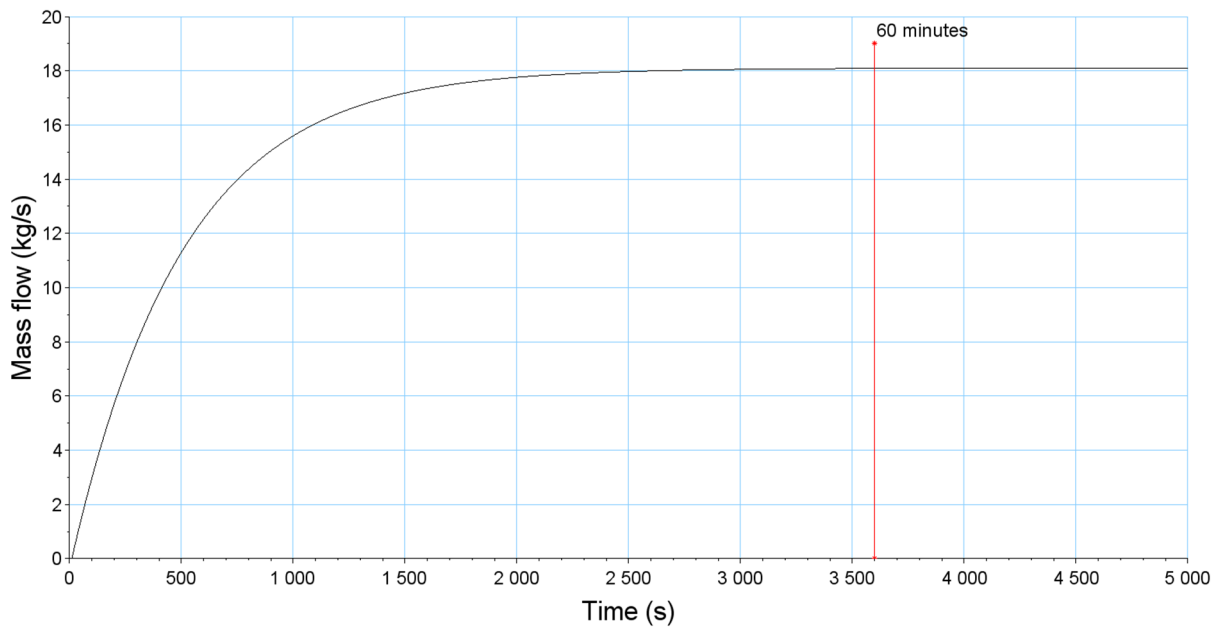


FIGURE 17: Simulation of production well flow

Since the model was focused on the hot end of the power plant, the condensing system was not included but it is still a crucial part of the start-up procedure. In these simulation scenarios the assumption is made that this aspect of the procedure has been properly carried out.

At 2,600 s (43 min.) the mass flow is 18.05 kg/s. 17 minutes later (at the 60 min. mark) the mass flow is 18.1 kg/s. The result converges to the expectation that the flow rate initially increases quickly when the well is opened until further opening (or reduction in pressure) cannot further increase the flow. Figure 18 shows the mass steam flow rate after separation.

In the model, the highest steam flow rate achieved was 11.76 kg/s compared to the actual mass flow of 11.8 kg/s. This is a realistic and acceptable result. Figure 19 shows separator pressure. The simulated

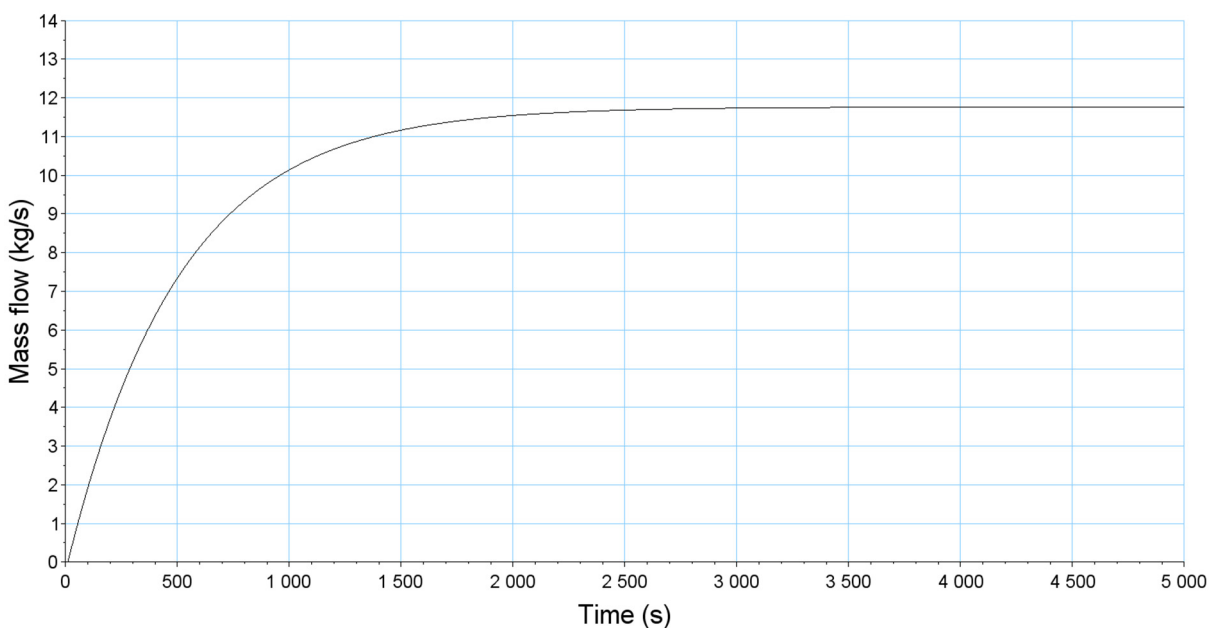


FIGURE 18: Simulation of mass steam flow after separation

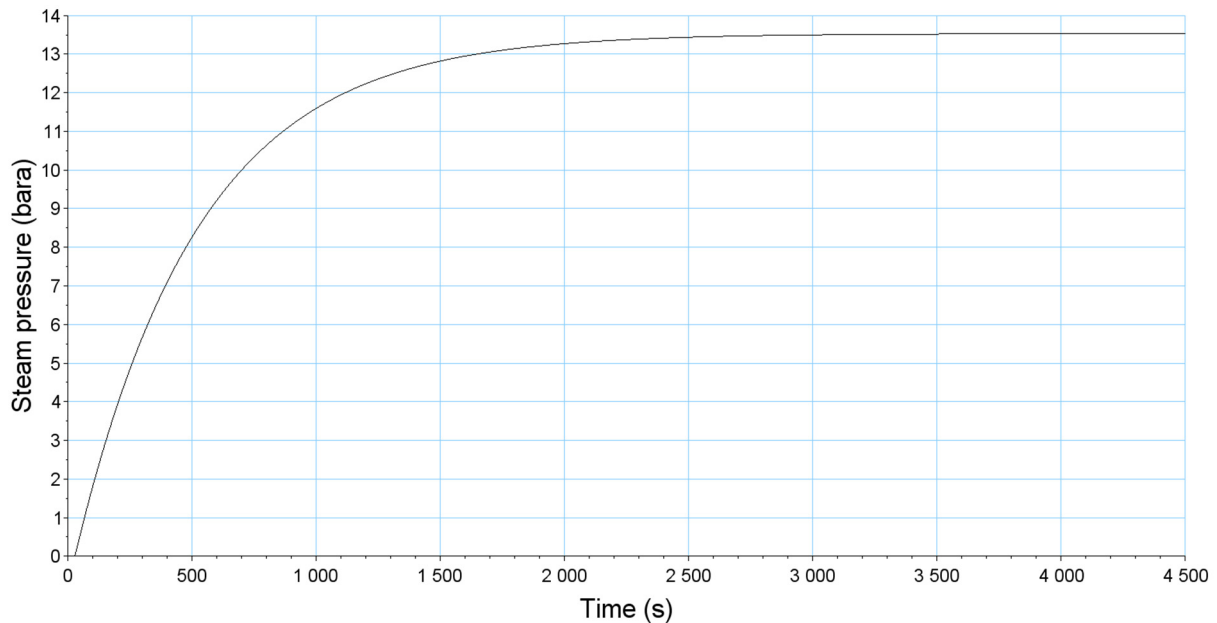


FIGURE 19: Simulation of separator pressure

pressure after taking into account the pressure losses is negligible.

Once the steam lines have warmed up and the turbine has been rotated sufficiently using the barring gear, the main steam isolation valve is opened followed by the governor control valve. Steam is admitted into the turbine until it achieves rated speed (in this case 5845 rpm). At this point the generator is synchronised to the grid and given an initial power output (load) of 500 kW. After several minutes (usually ten, to allow generator heat soak), the power output is increased stepwise until it reaches the final output of 5.2 MW. Figure 20 neglects the step-wise increase of power output and assumes that the operator increases the power output to full load immediately after synchronisation. This is sometimes done when the machine has been running and the generator trips and is re-synchronised quickly. The simulated results show one minute to reach full load. This is not exact but realistic enough.

In Figure 21 we see that the control valve opens to 16% in the same amount of time (60 s) that it takes to reach full load. This behaviour is divergent from the behaviour of the control valves in the actual power plant which are usually at least 50% open in order to attain a power output of 5.2 MW. It is evident from the simulated results that the control valve has a quick opening characteristic. Inlet control valves tend to have non-linear characteristics (Pondini et al., 2017) and the inherent characteristic of most valves change during operation where a valve with an inherent linear curve may resemble a quick opening characteristic and one with an equal percentage curve resembles a linear curve. However, a quick opening characteristic is not best suited for modulating valves. The operational part of the valve is limited in that case because maximum output is achieved by a very small opening.

## 4.2 Changing the set-point of the power output

A simulation was carried out to see the response when the set-point is changed from the nominal power output of 5.2 MW to both a lower and a higher set-point.

### 4.2.1 Set-point change to 4.4 MW

Figure 20 shows lowering of the set-point to 4.4 MW.

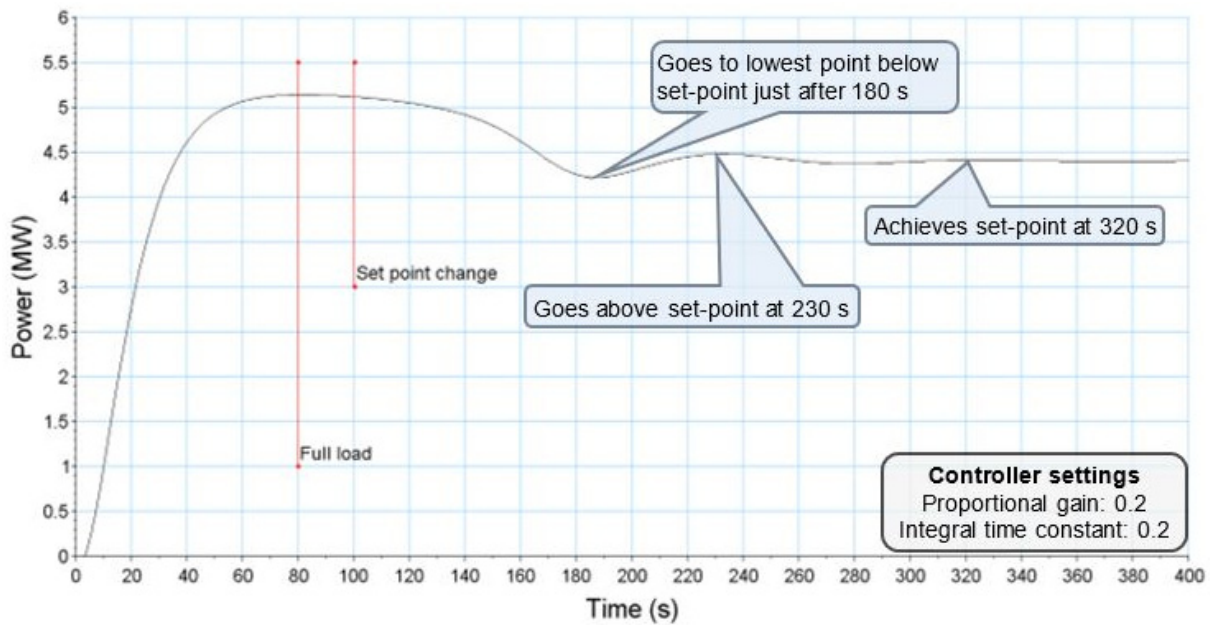


FIGURE 20: Simulation showing set-point change of power output

The load change occurs due to the feedback signal that is sent to the controller. As explained in Section 3.4.7, a comparison is made between the set-point and the feedback signal causing closing of the control valve until the set-point has been reached. The model produces good results reducing the generator output to match the set-point. Figure 21 shows the behaviour of the valve when the set-point change occurs.

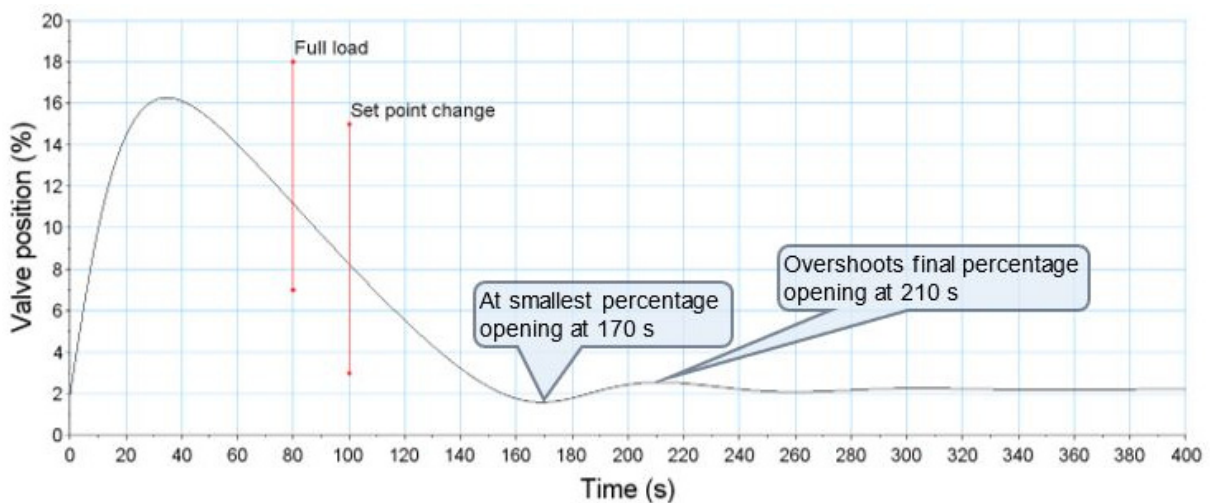


FIGURE 21: Control valve response during set-point change to 4.4 MW

The control valve closes to match the lower set-point. However, given that the generator output can be 4.4 MW with a valve opening of 2%, it is evident that the model of the control valve is not a true representation of the actual control valve. Figure 22 shows how the turbine inlet pressure changed as the control valve responded to the controller. The response matches what would happen in a real life situation.

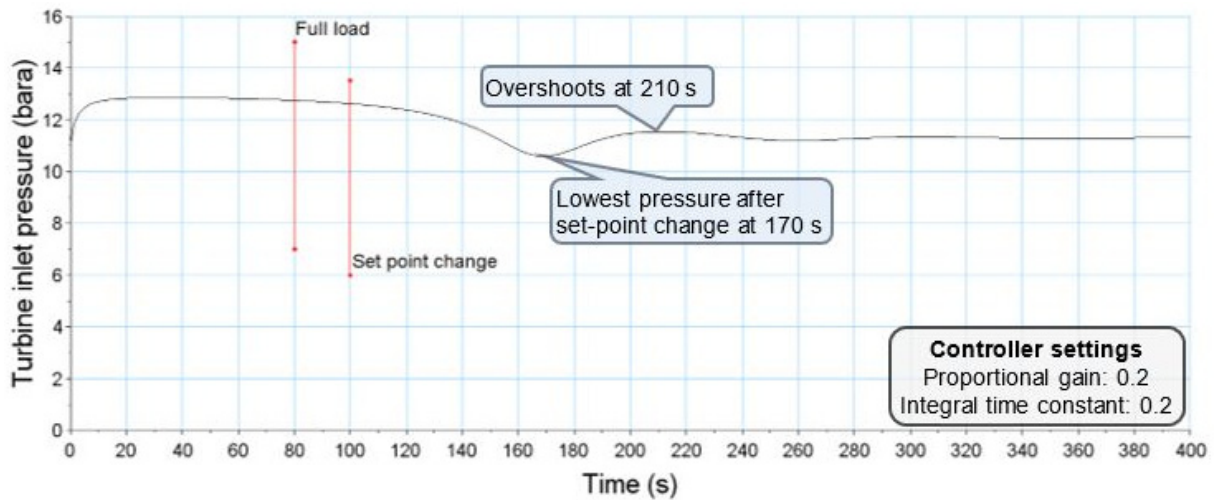


FIGURE 22: Changes in turbine inlet pressure in response to control valve response

#### 4.2.2 Set-point change to 5.3 MW

The set-point was changed from the nominal 5.2 to 5.3 MW. From the perspective of the model, this is beyond the turbine's capability. Figure 23 shows the behaviour of the control valve. It keeps opening to take in more steam and increase the load. Since the error between the set-point and feedback remains constant it continues to open. This is a reasonable response to the set-point change and shows that despite the flaws in the modelling of the control valve it can still deliver a response that matches reality.

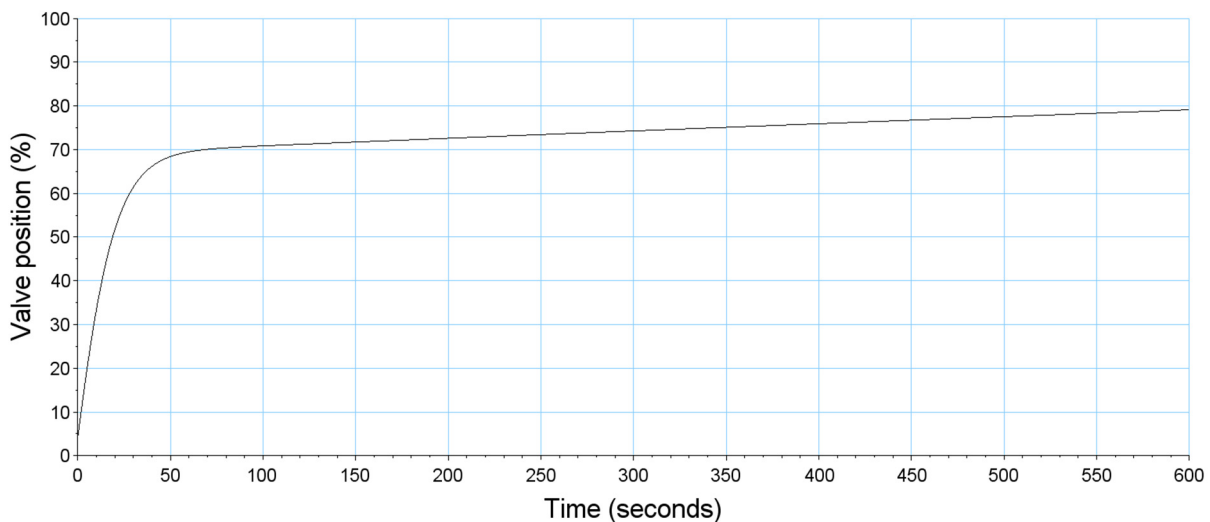


FIGURE 23: Control valve response during set-point change to 5.3 MW

#### 4.3 Adjustment of controller parameters

In Figures 20-22, both the proportional and integral gains were set to 0.2. Figures 24-26 show a scenario where the gains are set to 0.4. Comparing the response to different controller settings, we can see from Figure 20 that the response takes longer with the lower proportional gain, reaching 4.2 MW 80 seconds after the set-point change occurs. In comparison, the response is 20 seconds faster with the higher proportional gain (Figure 24), but only reaches a value of 3.9 MW. This is a typical response which can lead to oscillations that can cause instability in the system. The purpose of the integral time constant is to correct the steady state error over time. It reduces oscillations but causes overshoots. A certain level

of overshooting past the set-point has to occur to allow the system to respond quickly. Usually, the optimum P and I parameters are achieved through a process of trial and error.

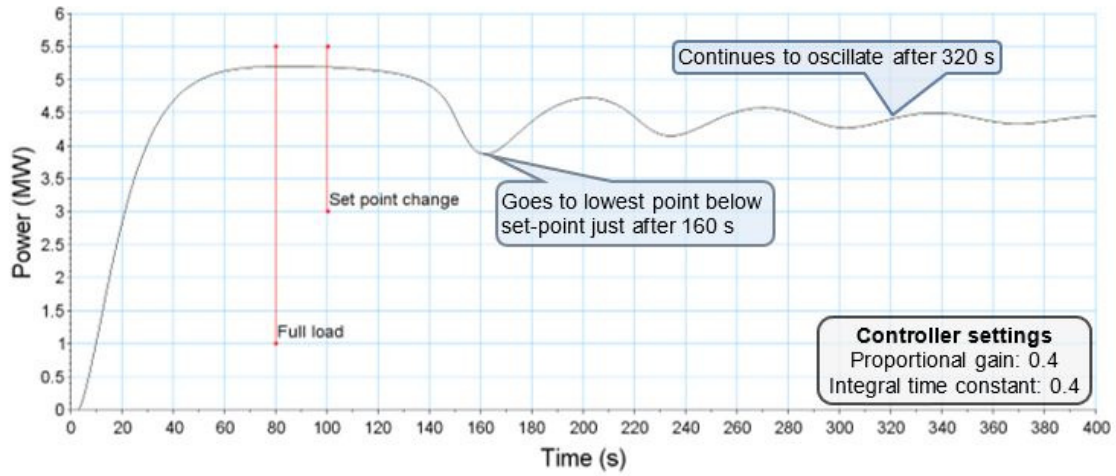


FIGURE 24: Simulation showing set-point change of power output

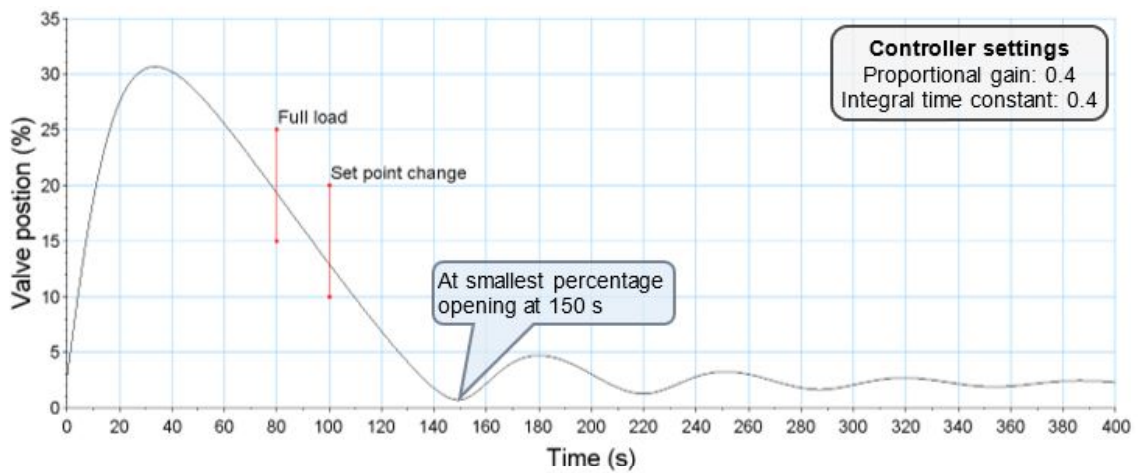


FIGURE 25: Control valve response to set-point change with different controller parameters

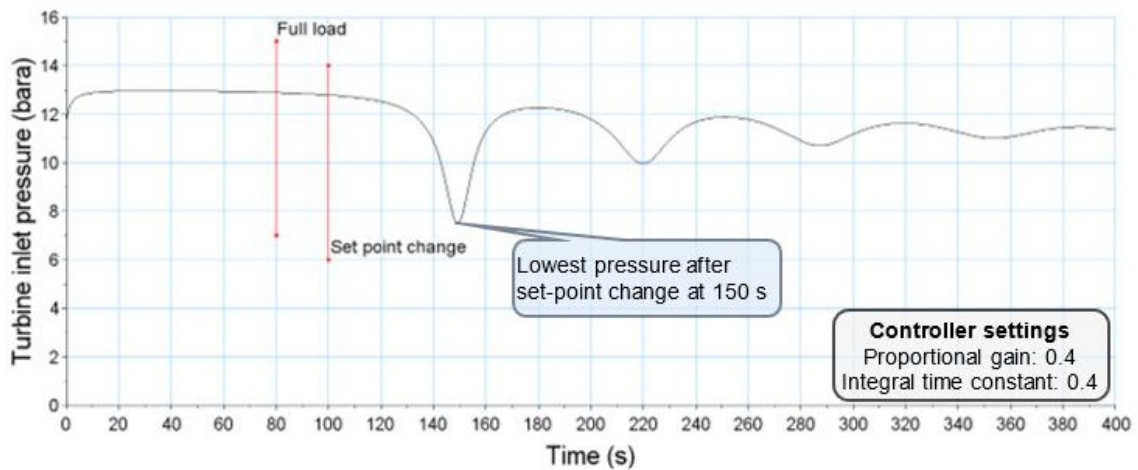


FIGURE 26: Changes in turbine inlet pressure in response to control valve response



In Figure 25 the control valve responds faster and more aggressively than in Figure 21. It is also worth noting that in both cases the control valve reaches its lowest opening 10 seconds before the generator output as would be expected in a real application.

In Figure 26 it can be observed that the turbine inlet pressure reaches a value of 7.5 bar-a compared to Figure 22 where the lowest pressure is 10.5 bar-a. The low pressure in Figure 26 can be attributed to the control valve opening of 1%. Overall, the response of the model to changes of set-point with different controller parameters is not exact but realistic.

## 5. CONCLUSIONS

- The project sought to create a foundation for the development of a training simulator for the wellhead power plants in Olkaria, Kenya. The need for a training simulator has been explained as well as the process required to develop one.
- A model of the hot end of the power plant has been developed using mathematical equations and the Xcos module of the software Scilab. Three typical simulation scenarios have been carried out and the results presented and discussed. From the results it is evident that the response of the model developed has a high degree of conformance with the actual wellhead power plant and can form a strong foundation for further modelling works.
- One major shortcoming was the control valve characteristic that to a certain extent diverged from reality. Even though the generator model delivered good results, it is extremely simplified and may not be able to produce realistic results when subjected to more complex simulation scenarios.
- It should be noted that depending on training requirements it is not always necessary to have a simulator that matches the power plant in its entirety. It is sufficient to have a simulator that can meet the specific training needs.
- In the case of this project the model can be used to run a simulator that trains operators on start-up and changes in load and can assist the maintenance team in optimising controller parameters.

## 6. RECOMMENDATIONS

- It is vital that the simulation is developed further by verifying certain values such as estimated dimensions and constants. They should be adjusted and measurements taken where necessary.
- Further development of the generator model and control valve are necessary.
- In order to complete the simulator development the following is required:
  - Inclusion of the pressure control and brine level control valve to the hot end of the model.
  - Modelling of the cold end of the power plant: the condenser, gas extraction system and cooling water system.
  - Completion of the user interface and integration with the model in order to create an interactive window.

## ACKNOWLEDGEMENTS

I thank my employer KenGen for granting me the opportunity to attend this programme. I appreciate the assistance offered at different stages of the programme by the UNU-GTP team: the director Mr Lúdvík S. Georgsson, deputy director Mr Ingimar G. Haraldsson, Ms Málfríður Ómarsdóttir, Mr Markús A. G. Wilde and Ms Thórhildur Ísberg.

Many thanks to my supervisor Dr Páll Valdimarsson for his guidance, for pushing me out of my comfort zone, renewing my passion for engineering and bringing out the best in me.

Special thanks to my family, particularly my parents for their prayers, my sister for her encouragement and especially my wife Emma and daughter Lulu for their patience and full support. I also thank my friends and colleagues for cheering me on through the entire process.

Last but not least, I want to acknowledge all the UNU-GTP fellows who made my stay in Iceland pleasant and the geothermal utilisation team Adhiguna Satya and Laura Cordero for their encouragement and advice during the project work.

I am grateful to God for providing me with the health, strength and peace of mind during the course of this programme.

## REFERENCES

Apiyo, W., 2016: Centralised monitoring and control dispatch centre for the geothermal wellhead power plants in Kenya. Report 9 in: *Geothermal training in Iceland 2016*. UNU-GTP, Iceland, 27-62.

Bell, I. H., Wronski, J., Quoilin, S. and Lemort, V., 2014: Pure and pseudo-pure fluid thermophysical property evaluation and the open-source thermophysical property library CoolProp. *Industrial & Engineering Chemistry Research*, 53-6, 2498-2508. Software available on: [www.coolprop.org](http://www.coolprop.org).

Chaibakhsh, A., and Ghaffari, A., 2008: Steam turbine model, *Simulation Modelling Practice and Theory*, 16, 1145-1162.

Cooke, D.H., 1985: On prediction of off-design multistage turbine pressures by Stodola's ellipse, *J. Eng. Gas Turbines Power*, 107-3, 596-606.

DiPippo, R., 2005: *Geothermal power plants: principles, applications and case studies*. Elsevier Advanced Technology, Oxford, UK, 450 pp.

Dulau, M. and Bica, D., 2014: Mathematical modelling and simulation of the behaviour of the steam turbine. *Procedia Technology*, 12, 723-729.

Garrido, J., Zafra, Á. and Vázquez, F., 2009: Object oriented modelling and simulation of hydropower plants with run-of-river scheme: A new simulation tool. *Simulation Modelling Practice and Theory*, 17-10, 1748-1767.

Hrdlicka, P., Neuman, P., and Sulc, B., 2002: Process instrumentation modular models of thermal power plant for operator training simulators. *IFAC Proceedings*, 35-1, 437-442.

Hubel, M., Meinke, S., Marcus A., Wedding, C., Nocke, J., Glerow, C., Hassel, E., and Funkquist, J., 2017: Modelling and simulation of a coal-fired power plant for start-up optimisation. *Applied Energy*, 208, 319-331.

ISA, 1993: *Fossil fuel power plant simulators – functional requirements. ANSI/ISA-77.20-1993*, Instrument Society of America, USA, 43 pp.

KenGen, 2015: *C50 operation & maintenance manual*. Kenya Electricity Generating Company, Ltd. – KenGen.

Kim, T.S., Park, H.J. and Ro, S.T., 2001: Characteristics of transient operation of a dual-pressure bottoming system for the combined cycle power plant. *Energy*, 26-10, 905-918.

Ogata, K. 2010: *Modern control engineering* (5<sup>th</sup> ed.). Prentice Hall, NJ, USA, 894 pp.

Pondini, M., Colla, V., and Signorini, A., 2016: Models of control valve and actuation system for dynamics analysis of steam turbines. *Applied Energy*, 207, 208-217.

Sanchez, E., Torres, C.F., Guillen, P., and Larrazabal, G., 2013: Modeling and simulation of the production process of electrical energy in a geothermal power plant, *Mathematical and Computer Modelling*, 57, 2140-2148.

Scilab Enterprises, 2012: *Scilab: free and open source software for numerical computation*. Scilab, website: [www.scilab.org](http://www.scilab.org).

Stemmet, L., and Ahmed, M.D, 2015: The decision maker's cognitive load (Chapter 635). In: Category Psychology and Human Behaviour. In: Khosrow-Pour, M., *Encyclopaedia of information science and technology* (3<sup>rd</sup> ed.). Information Resource Management Association, USA, 6466-6474.

Tomschi, U., Jackisch, H., and Newald, R., 2006: Operator guidance simulator: a new power plant training tool concept. *Proceedings of the 5<sup>th</sup> IFAC Symposium on Power Plants and Power Systems Control, IFAC Proceedings*, 39-7, 327-332.

Vieira, M.F.Q., Neto, J.A.N., Scaico, A., Santoni, C., and Mercantini, J.M., 2010: A Real-time interface simulator for operator training: a proposed architecture. *Simulation*, 86-1, *Society for Modeling and Simulation International*, 53-63

## APPENDIX I: Program written in Scilab for testing of steady state operation

### Colebrook-White function

```
function f=colebrook_v00(Re, relroughness)
// Version v00 2018-03-01
change = 1 ;
tolerance = 1e-6 ;
f = 0.02 ;
ii=0 ;
while change>tolerance
ii = ii + 1 ;
f_old = f ;
f = 1/(4 * log10(relroughness/3.7+2.51/(Re*sqrt(f)))^2) ;
change = 2 * abs(f_old-f) / (f_old+f)
end
endfunction
```

### Script used for steady state testing of power plant model

```
// 1. Production well
T_reservoir = 281.5 ;
```

```
M_dot_well = 18.1 ;
X_well = 0.65 ;
```

```
// 2. Separator
```

```
L_brine = 0.41 ; // Different switch levels LL: 0.28, L: 0.35, N: 0.41, H: 0.53, HH: 0.68
L_separator = 1.0 ; // Estimated. Actual dimensions not confirmed
A_separator = 2.9 ; // Estimated. Actual dimensions not confirmed
V_separator = L_separator * A_separator ;
V_steam = (L_separator - L_brine) * A_separator ;
V_brine = V_separator - V_steam ;
M_steam = M_dot_well * X_well ;
M_brine = M_dot_well * (1 - X_well) ;
rho_steam = rho(2) ;
rho(2) = M_steam / V_steam ;
P_separator = P(2) ;
P(2) = Props('P', 'D', rho(2), 'Q', 1, 'Water') ;
```

```
// 3. Steam pipeline
```

```
L = 15 ; // Estimated pipe length
D(3) = 0.3556 ; // Pipe diameter in metres (14 inches). From P&I drawings
Q(3) = M_steam / rho(2) ;
A(3) = (%pi*D(3)^2)/4 ;
Velocity(3) = Q(3) / A(3) ;
mu = Props('V', 'T', 193, 'Q', 1, 'Water') ; // Viscosity
rho(3) = Props('D', 'T', 193, 'Q', 1, 'Water') ; // Density of steam after separator before strainer
v = mu / rho(3) ; // Kinematic viscosity
Re = (Velocity(3) * D(3))/v ; // Reynolds number
Roughness_abs = 1E-3 ; // Absolute roughness in metres
Roughness_rel = Roughness_abs / D(3) ; // Relative roughness
f = colebrook_v00(Re, Roughness_rel) ; // Friction factor calculated using Colebrook-White equation
P_friction = ((L * f * Velocity(3)^2 * rho(3)) / (2 * D(3))) * 1E-5 ; // in bar
P(3) = P(2) - P_friction ;
```

```
// 4. Governor Control valve
```

```
rho(4) = Props('D', 'T', 192.3, 'Q', 1, 'Water') ; // Density of steam after strainer
Q(4) = M_steam / rho(4) ;
D(4) = 0.1524 ; // 6 inch control valve
A(4) = ((%pi*D(4)^2)/4) ;
Velocity(4) = Q(4) / A(4) ;
P_loss = 0.5E5 ; // Pressure drop in bar. From rated conditions. Some commissioning data show up to 4 bara
k_1 = (2 * P_loss) / (rho(4) * Velocity(4)^2) ;
for i = 1:101
    rho(i) = Props('D', 'P', P(3), 'Q', 1, 'Water') ;
    x(i) = i-1 ;
    k_lmin = k_1 ;
    P4(i) = -(k_lmin * Velocity(4)^2 * rho(i) - 2e5 * P(3) * x(i)) / (2e5 * x(i)) ;
end
```

```
// 6. Generator
```

```
V = 11 ; // Terminal voltage
U = 0.110 ; // Excitation voltage
del = 30 ; // Rotor angle
Xd = 1.1 ; // Direct axis synchronous reactance
Pe = (U * V / X) * abs(sin(del)) ;
Pm = 6.5 ;
P = Pm - Pe ;
```